ChemPubSoc Europe

DOI: 10.1002/batt.201900117

BATTERIES & SUPERCAPS Communications

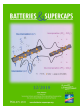

Successive Cationic and Anionic (De)-Intercalation/ Incorporation into an Ion-Doped Radical Conducting Polymer

Heng Chen,[a] Chengyang Xu,[a] Yadi Zhang,[a] Mufan Cao,[a] Hui Dou,*[a] and Xiaogang Zhang*[a]

The further development of conducting polymers (CPs) as electrode materials is restricted by the limited doping level, solely ionic reaction as well as the insufficient reversibility and stability. In order to overcome the deficiency of intrinsic properties, a combined strategy is adopted to modify a p-type CP (polythiophene, PTh) through grafting a radical pendant (2,2,6,6-tetramethylpiperidinyl-1-oxyl, TEMPO) and incorporating a redox-active dopant ($Fe(CN)_6^{3-}$) into the π-conjugated backbone of PTh. TEMPO group works as the electron donor allowing anionic incorporation (PF_6^-, ClO_4^-) and $Fe(CN)_6^{3-}$ doping in the conducting matrixes of PTh combines with cations (Li^+) to deliver extra capacity, leading to the final composite shows a successive cationic and anionic (de)-intercalation behavior. This dual-ion transportation mechanism of $Fe(CN)_6^{3-}$ doped P(Th-TEMPO) facilitates the enhanced electrochemical performance, including two significant voltage plateaus (3.6 V and 2.9 V), a reversible capacity from 76 mAh g^{-1} to 135 mAh g^{-1} at an ultra-high coulombic efficiency (more than 99%), which result in a high energy density.

Redox-active π-conjugated conducting polymers (CPs) are increasingly crucial for a new generation of energy storage systems (ESSs), owing to their fast electron transportability, abundant redox-active sites and electro-optical properties.[1] However, most of π-conjugated CPs such as polypyrrole (PPy) and polythiophene (PTh), show a typical p-type behavior with the doped anions as charge-balancing ions in the polymer network.[2] When p-type CPs are applied as the electrode materials, their limited doping level of anions may lead to a comparatively low discharge capacity, an insufficient coulombic efficiency as well as the poor cycling performance due to a diffusive dissolution of the anions to the electrolyte.[3] Simultaneously, the low redox potential and environmental instability of intrinsic n-type CPs also reduce the possibility of their application in ESSs.[4]

In fact, in order to further improve the electrochemical properties, the rational molecular designs are the key to overcome the intrinsic deficiency of π-conjugated CPs.[5] Generally, when hole-transporting (semi)conducting polymers (p-type) are oxidized or electron-hopping polymers (n-type) are reduced, the electronic conductivity could be significantly improved owing to doped mobile counterions.[6] The different molecular species play a role as an electron donor or acceptor to change the carrier concentrations and band gap of CPs, greatly enhancing the electron conductivity and electrochemical stability of polymers.[7] Therefore, doping strategy is often used to introduce organic/inorganic species into a polymer network. If these inserted molecular species are redox-active, the doped polymer can provide more abundant redox sites as well as adjustable redox potentials.[8]

There are two effective strategies to modify CPs with functional molecular species for the better electrochemical performance in rechargeable batteries. One feasible way is to graft redox-active organic pendant groups such as quinone and nitroxide radicals, onto the π-conjugated backbone of CPs.[9] The superior redox activity of these pendant groups can provide fast charge transfer kinetics, extra reversible capacity by facilitating the electron transportation and ion doping of the whole polymer. The other one is to incorporate redox-active dopants into CPs matrixes via copolymerization and doping strategies as mentioned above.[10] The anionic dopants such as ferrocyanide [$Fe(CN)_6^{4-}$],[8] indigo carmine (IC)[11] as well as polyoxometalate (POM),[12] are effectively trapped within the polymeric matrix with reversible redox chemistry. These anchored species can work as the electron acceptors and convert the ion transportation mechanism of intrinsic p-type CPs into a stable cation-(de)insertion behavior. So far, there are many reports introducing the aforementioned strategies to modify thiophene-based polymers as the electrode materials, neither of which could combine the reversible capacity and cycling performance at the same time.[13] Non-redox activities of dopants, weak insolubility and single cation participant reaction are the possible reasons.

To obtain both high power and energy density, we adopt a combined strategy that fabricating an anion-doped radical polythiophene (PTh) on the carbon nanotube (CNT) surface. Firstly, the nitroxide radicals, 2,2,6,6-tetramethylpiperidine-1-oxyl (TEMPO), is grafted to form the composite monomer Th-TEMPO. Batteries with radical polymers show fast electrochemical kinetics, good cyclabilities and power density.[14] The redox-active anionic dopant, $Fe(CN)_6^{3-}$, is then introduced into

[a] H. Chen, C. Xu, Y. Zhang, M. Cao, Prof. H. Dou, Prof. X. Zhang
Jiangsu Key Laboratory of Electrochemical Energy Storage Technologies,
College of Material Science and Technology,
Nanjing University of Aeronautics and Astronautics,
Nanjing 210016, P.R. China
E-mail: dh_msc@nuaa.edu.cn
azhangxg@nuaa.edu.cn

Supporting information for this article is available on the WWW under https://doi.org/10.1002/batt.201900117

the P(Th-TEMPO) network via secondary doping process after electrochemical polymerization. Because of the closing redox potential to the fermi level of PTh, $Fe(CN)_6^{3-}$ work as the counterion dopant to ensure the electronic conductivity of the polymer and function as the redox meditator to facilitate the charge transportation, which is available and stable.[8] The final composite of $Fe(CN)_6^{3-}$ doped P(Th-TEMPO)/CNT shows a successive anionic and cationic co-reaction behavior since TEMPO group works as an electron donor allowing anionic (de)-incorporation when it is oxidized and small cations insert into the polymer when $Fe(CN)_6^{3-}$ is reduced. This dual-ion transportation mechanism is definitely demonstrated by in situ electrochemical measurements of Fourier transform-infrared spectrometer measurements (FTIR) and the electrochemical quartz crystal microbalance methods (EQCM). Furthermore, when this composite is adopted as the free-standing electrode in Li-ion batteries, better electrochemical performances including an enhanced discharge capacity, an ultra-high coulombic efficiency and a good cycling performance, are significantly achieved.

Th-TEMPO was firstly synthesized via a esterification reaction between 3-thiophenecarboxylic acid and 4-hydroxy-TEMPO in the presence of 4-dimethylaminopyridine (DMAP) and N,N′-dicyclohexylcarbodiimide (DCC) in dichloromethane (DCM), as presented in Figure 1.[13b] The as-synthesized Th-

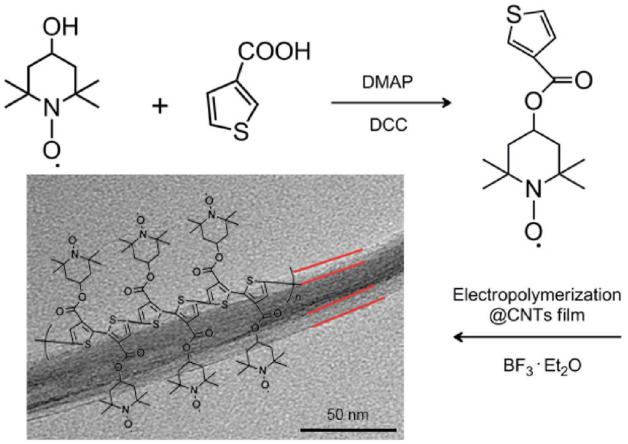

Figure 1. Synthesis route of Th-TEMPO and P(Th-TEMPO).

TEMPO was confirmed by ^1H NMR spectroscopy and FTIR methods (specific analysis in Figure S1). Th-TEMPO was then electropolymerized (Figure S2) through cyclic voltammetry in boron fluoride-ethyl ether (BFEE) solution.[15] When the electrochemical polymerization was carried out, the intensity of the oxidation and reduction current increased continually during every sweep, confirming the polymer grew and deposited onto the CNTs film. The homogeneous coating layer, showing a thickness of about 7 nm on the CNTs, is clearly visible in the transmission electron microscope (TEM) image (Figure 1).

$Fe(CN)_6^{3-}$ was doped into the P(Th-TEMPO) matrixes via a controllable electrochemical method.[16] The doping process was dealt with the potentiostatic methods in the aqueous solution with $Fe(CN)_6^{3-}$ ions as the redox-active additions and PO_4^- ions as the assist dopants (Figure S3). We firstly set a negative potential to output the former doping ions absolutely at −0.25 V vs. Ag/Ag^+; then, two doping processes were realized at 0.8 V and 0.9 V vs. Ag/Ag^+ with more than 10 min to ensure the functional P(Th-TEMPO) reaching at a high doping level, which is 1.4 tested by X-ray photoelectron spectroscopy (XPS) (Figure S4). Compared to N 1s XPS spectra of the undoped P(Th-TEMPO) (Figure S4b), a new peak at 398 eV appeared in that of $Fe(CN)_6^{3-}$-doped P(Th-TEMPO) (Figure S4c) corresponding to the N element of $Fe(CN)_6^{3-}$ without the shift of peaks of TEMPO at 401.0 eV and 402.5 eV. It should be mentioned that the quickly electrochemical polymerization may cause a partial oxidation, which cause the TEMPO moieties presenting 2 different redox state (401.0 eV for TEMPO, 402.5 eV for $TEMPO^+$).[17] We calculated the doping level according to the relative areas ratio of peaks for the two kinds of N element (1.4), which is equally regarded as the molar ratio between thiophene monomers and $Fe(CN)_6^{3-}$ ions.

P(Th-TEMPO) and $Fe(CN)_6^{3-}$-doped P(Th-TEMPO) electrode show different redox behaviors with respective ion transportation mechanism. As shown in Figure 2a, the undoped polymer exhibits reversible redox couples at around 0.65 V vs. Ag/Ag^+, corresponding to the oxidation and reduction of TEMPO with the p-type (de)-incorporation of anions (ClO_4^-, PF_6^-).[13a,18] The doped polymer shows bigger additional redox peaks at about 0 V indicating of a reversible $Fe(CN)_6^{3-}/Fe(CN)_6^{4-}$ redox couple. The similar result is discovered in the galvanostatic charge-discharge curves of undoped and doped P(Th-TEMPO) (Figure 2b) at a current density of 0.2 A g^{-1}. Two reversible voltage plateaus of doped P(Th-TEMPO) owe to respective redox reactions of TEMPO and $Fe(CN)_6^{3-}$, whereas a short plateau above 3.6 V of undoped P(Th-TEMPO) is only contributed by the TEMPO group. Herein, we assumed a dual-ion transportation mechanism was included in the doped P(Th-TEMPO) electrode (Figure 2c). Taking the discharging process for example, the anionic (PF_6^-, ClO_4^-) de-incorporation from the skeleton of TEMPO groups is firstly realized when $TEMPO^+$ begin to be reduced. When discharged to the lower plateau, the solvated cations (Li^+) insert the electrode with the reduction of $Fe(CN)_6^{3-}$ ions after de-solvation. There is a reversible ion transportation process on charge, accompanied by the cations extracting at low voltages and anions intercalating at high voltages.

These two electrodes and pure CNTs film were fabricated in LIBs for further research. With a p-doping mechanism, the undoped P(Th-TEMPO) delivers a capacity of 76 mAh g^{-1} (Figure 2b) with an insufficient coulombic efficiency below 85% (Figure 3c), showing a limit doping level for the anionic incorporation. In contrast, it is easy to discover a great enhancement in the reversible capacity of the doped P(Th-TEMPO) is derived from the contribution of redox properties of $Fe(CN)_6^{3-}$ ions, where the CNTs contribute the capacity of 14 mAh g^{-1} via Faradaic reaction (Figure S5). Especially, an ultra-high efficiency (Figure 3c) more than 99% for the doped P(Th-TEMPO) is obtained owing to the interaction between CPs and doping ions, which decrease the obstacle for ionic trans-

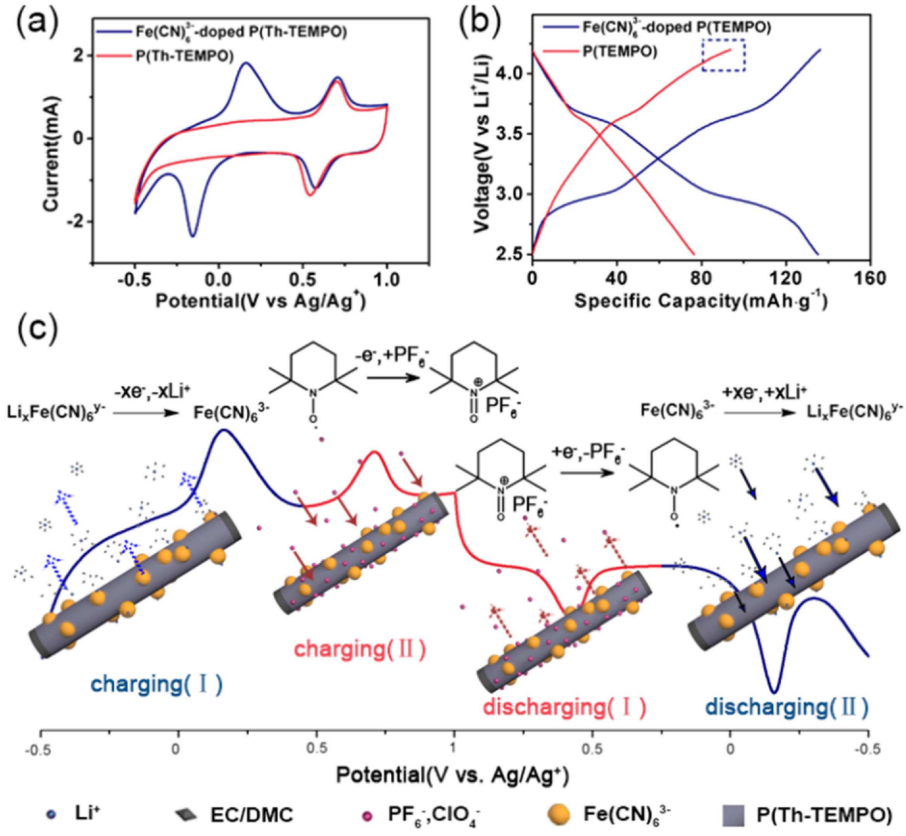

Figure 2. (a) Cyclic voltammetry (20 mV s^{-1}) of P(Th-TEMPO) (red) and $Fe(CN)_6^{3-}$-doped P(Th-TEMPO) (blue) in 0.1 M $LiClO_4$/acetonitrile solutions; (b) Galvanostatic charge and discharge curves of P(Th-TEMPO) (red) and $Fe(CN)_6^{3-}$-doped P(Th-TEMPO) (blue) with the electrolyte of 1 M $LiPF_6$ EC/DMC; (c) Possible charging and discharging processes of the doped P(Th-TEMPO).

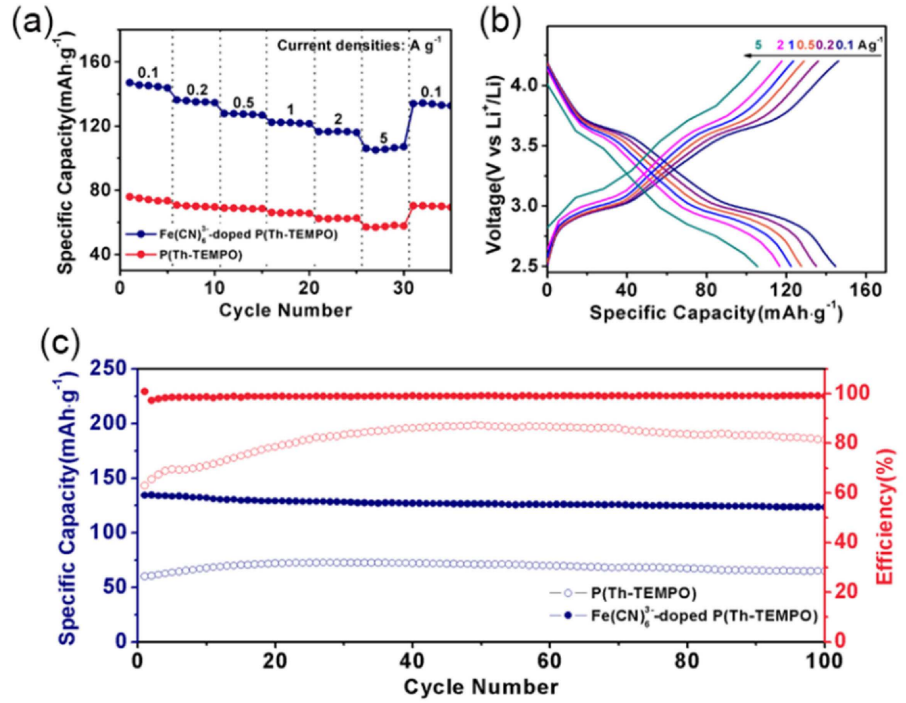

Figure 3. (a) Rate performances at different current densities; (b) Galvanostatic charge and discharge curves of $Fe(CN)_6^{3-}$-doped P(Th-TEMPO) at different current densities; (c) Cycling performances at the current density of 0.2 A g^{-1}.

portation and achieve an excellent reversibility of redox processes.[19] The discharge capacities and curves are obtained at different current densities (Figure 3a and 3b). With the supporting of CNTs and π-conjugated backbones, the polymer electrode exhibits an excellent rate performance, showing a fast kinetics process. However, to some extent, the intrinsically poor rate property of $Fe(CN)_6^{3-}$ causes a greater loss in capacity at a high rate than that in the undoped one. Both two polymers show a good cycling performance (Figure 3c) at 0.2 A g^{-1} with a favorable capacity retention. Electrochemical impedance spectroscopy (EIS) tests were recorded in Figure S6 and Table S1, which point out an improved conductivity in the $Fe(CN)_6^{3-}$-doped P(Th-TEMPO). As expected, the functional doping ions play a crucial role as stacks to support the CPs matrixes, greatly enhancing the electrochemical stability, reversibility and charging/discharging capacity.

To confirm our assumption, in situ FTIR (Figure 4) and EQCM methods (Figure 5) were used to observe dual-ion transportation mechanism of the doped P(Th-TEMPO). A modified battery with a diamond window for in situ FTIR, fabricated under the same conditions to the coin cells, was initially cycled several times to ensure the actual process when testing. The whole FTIR spectra are presented in Figure S7 when the battery is charged and discharged. When the battery was first charged to the first plateau (charging I), the intensity of peaks at 1063, 1150, 1266, 1720 cm^{-1} (blue region) decreased gradually and disappeared around 3.4 V. The blue region presented C=O stretching of ethylene carbonate (EC) and dimethyl carbonate (DMC) at 1720 cm^{-1}, the skeletal stretching of EC at 1063 and 1150 cm^{-1} and ν(C–O) of DMC at

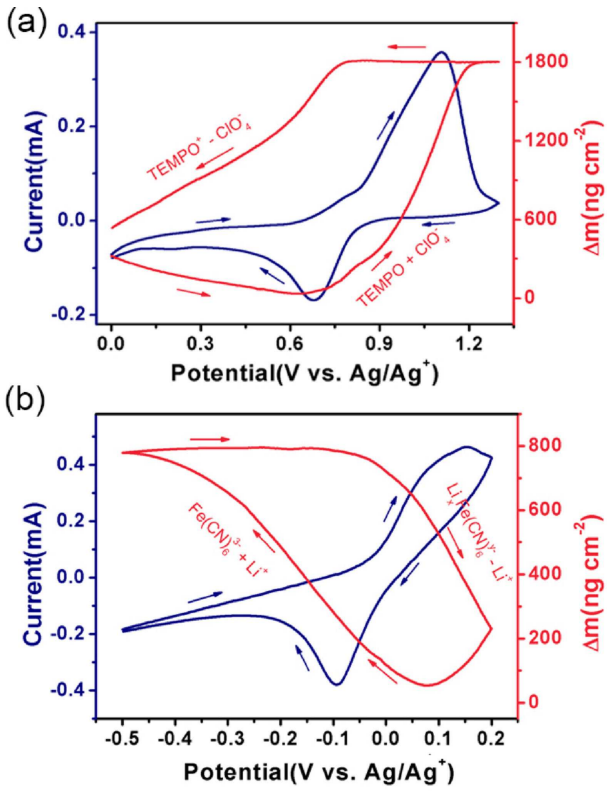

Figure 5. Gravimetric responses and corresponding voltammograms of $Fe(CN)_6^{3-}$-doped P(Th-TEMPO) in different voltage ranges for the respective investigation of TEMPO (a) and $Fe(CN)_6^{3-}$ ions (b).

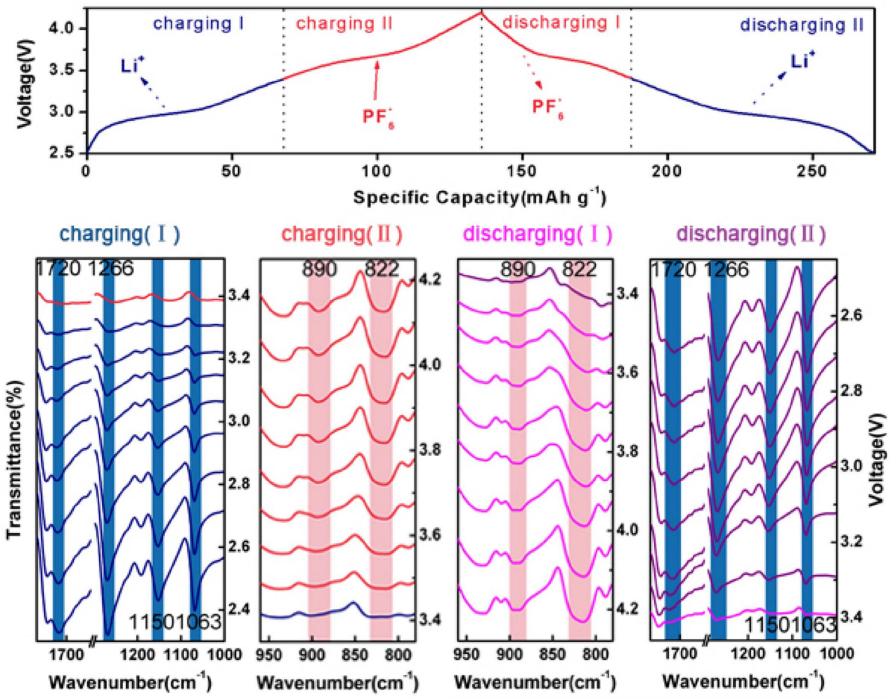

Figure 4. In situ FTIR spectra tested in 1 M $LiPF_6$ EC/DEC solution at a current density of 0.2 A g^{-1}: charging (I) (blue lines) from 2.5 V to 3.4 V (top); charging (II) (red lines) from 3.4 V to 4.2 V (top); discharging (I) (pink lines) from 4.2 V to 3.4 V (top); discharging (II) (purple lines) from 3.4 V to 2.5 V (top).

1266 cm^{-1}.[20] The variation of solvent molecules are related to the transportation of Li^+ ions by the effect of solvation.[21] Thus, the extraction of Li^+ ions, moving from cathode to anode after solvation, causes the decreasing number of solvent molecules. When charged to 4.2 V (charging II), we found two obvious peaks appeared at 890 and 822 cm^{-1} (red region) and strengthened continually corresponding to the characteristic vibration bands of PF_6^-, which indicated a large number of PF_6^- ions incorporated with the electrode when TEMPO was oxidized.[22] In addition, the N–O· signal is found at 1370 cm^{-1} and decreases gradually when charged, which exhibits the oxidation process of TEMPO groups.[9b] Correspondingly, with the discharging of the battery (discharging I), PF_6^- ions extracted from TEMPO groups and $TEMPO^+$ reduced, causing this two peaks at 890 and 822 cm^{-1} fade away and the peak at 1370 cm^{-1} appeared. When discharged from 3.4 V to 2.5 V (discharging II), solution molecules increased gradually accompanying Li^+ insertion after de-solvation.

Gravimetric responses (Figure 5) also confirmed our assumption that the doped P(Th-TEMPO) follows two redox processes. For better investigation of two redox reactions, we carried out EQCM tests at suitable voltage ranges respectively for TEMPO and $Fe(CN)_6^{3-}$. When doped P(Th-TEMPO) is oxidized at high potentials, the increase of the mass of electrode demonstrates the combination of anions (PF_6^-) and TEMPO groups with a typical p-type behavior (Figure 5a). Then, when the electrode is reduced at low voltages, the increase of mass is caused by the insertion of Li^+ ions into the electrode, accompanied by a fairly reversible process of the extraction of Li^+ ions when it is oxidized (Figure 5b). These EQCM results are in good agreement with the analysis of in situ FTIR, definitely confirming the dual-ion transportation mechanism. The equivalent molar mass (M) was obtained by the Faraday's law, displayed in Figure S8. When the doped polymer is oxidized, $Fe(CN)_6^{3-}$ releases a value of M at 8.57 g mol^{-1} possibly for the molar mass of Li^+ (6.94 g mol^{-1}) and solvent molecules, and TEMPO groups incorporates a value of M at 91.67 g mol^{-1} corresponding to the molar mass of ClO_4^- (99.5 g mol^{-1}). Similarly, a reversible redox process was obtained as respected. Simultaneously, ex situ mapping images of F element were presented in Figure S7. When the battery was charged to 4.2 V, the scan field (Figure S7a) was fully filled with F element (PF_6^-). With the reduction of $TEMPO^+$, a tendency was found that the content of F decreased at 3.4 V, well consistent with the result of in situ FTIR test. It needs to be said that the content of F at 3.4 V was almost the same to that at 2.5 V, indicating the absence of PF_6^- during the redox reaction of $Fe(CN)_6^{4-}$/$Fe(CN)_6^{3-}$.

Combining all of these ex situ and in situ results, we definitely demonstrate the $Fe(CN)_6^{3-}$-doped P(Th-TEMPO) follows a dual-ion transportation mechanism, that is a successive anionic and cationic (de)-insertion behavior during a full oxidation/reduction process. By using functionally anionic dopants and redox-active pendants, we successfully obtain a new form of CP free-standing electrode based on the moieties of electron acceptor and donor applied in LIBs, which exhibits great enhancements in reversibility, capacity, energy density and electrochemical stability. Our research provides an efficient strategy to design favorable organic-inorganic hybrid materials in LIBs, which could also extend to other applications in energy storage systems. Besides, there is a possibility that a multi-electron redox dopant in CPs to achieve better performances in ESSs.

Acknowledgements

H.C. and C.Y.X. contributed equally to this work. This work was supported by the National Natural Science Foundation of China (U1802256, 51672128, 21773118, 21875107), the Key Research and Development Program in Jiangsu (BE2018122), and a Project Funded by the Priority Academic Program Development of Jiangsu Higher Education Institutions (PAPD).

Conflict of Interest

The authors declare no conflict of interest.

Keywords: lithium-ion batteries · conducting polymer · organic cathode · doping strategy · dual-ion transportation

[1] a) J. Kim, J. H. Kim, K. Ariga, *Joule* **2017**, *1*, 739–768; b) T. B. Schon, B. T. McAllister, P.-F. Li, D. S. Seferos, *Chem. Soc. Rev.* **2016**, *45*, 6345–6404; c) M. Armand, J. M. Tarascon, *Nature* **2008**, *451*, 652.
[2] a) P. Novák, K. Müller, K. S. V. Santhanam, O. Haas, *Chem. Rev.* **1997**, *97*, 207–282; b) G. A. Snook, P. Kao, A. S. Best, *J. Power Sources* **2011**, *196*, 1–12.
[3] a) J. Xie, P. Gu, Q. Zhang, *ACS Energy Lett.* **2017**, *2*, 1985–1996; b) T. Shimidzu, A. Ohtani, T. Iyoda, K. Honda, *J. Electroanal. Chem. Int. Electrochem.* **1987**, *224*, 123–135; c) A. G. MacDiarmid, *Angew. Chem. Int. Ed.* **2001**, *40*, 2581–2590; *Angew. Chem.* **2001**, *113*, 2649–2659.
[4] a) Y. Liang, Z. Tao, J. Chen, *Adv. Energy Mater.* **2012**, *2*, 742–769; b) F. L. Klavetter, R. Grubbs, *Polycyclooctatetraene (polyacetylene): Synthesis and properties*, *Vol. 110*, **1988**.
[5] a) C. M. Lochner, Y. Khan, A. Pierre, A. C. Arias, *Nat. Commun.* **2014**, *5*, 5745; b) Z. Song, H. Zhou, *Energy Environ. Sci.* **2013**, *6*, 2280–2301.
[6] a) M. J. El, D. Mc Cullough, *Handbook of conducting polymers*, *Vol. 1*, **2007**; b) A. Pron, P. Rannou, *Prog. Polym. Sci.* **2002**, *27*, 135–190.
[7] a) M. Chabinyc, *Nat. Mater.* **2014**, *13*, 119; b) T. Le, Y. Kim, H. Yoon, *Polymers* **2017**, *9*, 150.
[8] M. Zhou, J. Qian, X. Ai, H. Yang, *Adv. Mater.* **2011**, *23*, 4913–4917.
[9] a) G. Li, S. Bhosale, S. Tao, S. Bhosale, J.-H. Fuhrhop, *J. Polym. Sci., Part A: Polym. Chem.* **2005**, *43*, 4547–4558; b) N. Casado, G. Hernández, A. Veloso, S. Devaraj, D. Mecerreyes, M. Armand, *ACS Macro Lett.* **2016**, *5*, 59–64; c) M. Yao, H. Senoh, T. Sakai, T. Kiyobayashi, *J. Power Sources* **2012**, *202*, 364–368; d) W. Choi, D. Harada, K. Oyaizu, H. Nishide, *J. Am. Chem. Soc.* **2011**, *133*, 19839–19843.
[10] a) G. Kickelbick, *Prog. Polym. Sci.* **2003**, *28*, 83–114; b) T. Rębiś, G. Milczarek, *Electrochim. Acta* **2016**, *204*, 108–117.
[11] a) H. K. Song, G. T. R. Palmore, *Adv. Mater.* **2006**, *18*, 1764–1768; b) S. Sen, S. Y. Kim, L. R. Palmore, S. Jin, N. Jadhav, E. Chason, G. T. R. Palmore, *ACS Appl. Mater. Interfaces* **2016**, *8*, 24168–24176.
[12] P. Gómez-Romero, M. Lira-Cantú, *Adv. Mater.* **1997**, *9*, 144–147.
[13] a) M. Aydin, B. Esat, *J. Solid State Electrochem.* **2015**, *19*, 2275–2281; b) M. Aydın, B. Esat, Ç. Kılıç, M. E. Köse, A. Ata, F. Yılmaz, *Eur. Polym. J.* **2011**, *47*, 2283–2294.
[14] a) K. Hatakeyama-Sato, H. Wakamatsu, R. Katagiri, K. Oyaizu, H. Nishide, *Adv. Mater.* **2018**, *30*, 1800900; b) K. Oyaizu, T. Kawamoto, T. Suga, H. Nishide, *Macromolecules* **2010**, *43*, 10382–10389.
[15] G. Shi, S. Jin, G. Xue, C. Li, *Science* **1995**, *267*, 994.
[16] C. Xu, L. Wu, S. Hu, H. Xie, X. Zhang, *iScience* **2019**, *14*, 312–322.

[17] Y. Li, Z. Jian, M. Lang, C. Zhang, X. Huang, *ACS Appl. Mater. Interfaces* **2016**, *8*, 17352–17359.
[18] C. Su, F. Yang, L. Xu, X. Zhu, H. He, C. Zhang, *ChemPlusChem* **2015**, *80*, 606–611.
[19] S. Yeol Kim, H.-K. Song, *Conducting Polymers with Functional Dopants and their Applications in Energy, Environmental Technology, and Nanotechnology*, *Vol. 21*, **2015**.
[20] a) Z. Osman, A. K. Arof, *Electrochim. Acta* **2003**, *48*, 993–999; b) C. L. Angell, *Trans. Faraday Soc.* **1956**, *52*, 1178–1183; c) Y. Ikezawa, H. Nishi, *Electrochim. Acta* **2008**, *53*, 3663–3669.
[21] K.-K. Lee, K. Park, H. Lee, Y. Noh, D. Kossowska, K. Kwak, M. Cho, *Nat. Commun.* **2017**, *8*, 14658.
[22] G. M. Begun, A. C. Rutenberg, *Inorg. Chem.* **1967**, *6*, 2212–2216.

Manuscript received: August 31, 2019
Accepted manuscript online: September 6, 2019
Version of record online: October 7, 2019